Development 138, 2935-2945 (2011) doi:10.1242/dev.065714

Sclerotome-derived Slit1 drives directional migration and differentiation of Robo2-expressing pioneer myoblasts

Osnat Halperin-Barlev and Chaya Kalcheim*

SUMMARY

Pioneer myoblasts generate the first myotomal fibers and act as a scaffold to pattern further myotome development. From their origin in the medial epithelial somite, they dissociate and migrate towards the rostral edge of each somite, from which differentiation proceeds in both rostral-to-caudal and medial-to-lateral directions. The mechanisms underlying formation of this unique wave of pioneer myofibers remain unknown. We show that rostrocaudal or mediolateral somite inversions in avian embryos do not alter the original directions of pioneer myoblast migration and differentiation into fibers, demonstrating that regulation of pioneer patterning is somite-intrinsic. Furthermore, pioneer myoblasts express Robo2 downstream of MyoD and Myf5, whereas the dermomyotome and caudal sclerotome express Slit1. Loss of Robo2 or of sclerotome-derived Slit1 function perturbed both directional cell migration and fiber formation, and their effects were mediated through RhoA. Although myoblast specification was not affected, expression of the intermediate filament desmin was reduced. Hence, Slit1 and Robo2, via RhoA, act to pattern formation of the pioneer myotome through the regulation of cytoskeletal assembly.

KEY WORDS: Avian embryo, Desmin, Dermomyotome, MyoD, Myf5, Myotome, Myofiber patterning, Rho GTPases, Somite

INTRODUCTION

Vertebrate muscles develop from somites, transient epithelial structures which, in response to environmental signals, dissociate to form the dermomyotome (DM) and sclerotome (Scl) (Christ and Ordahl, 1995). Although the DM contributes to most myotomal fibers (Christ et al., 1978; Cinnamon et al., 2006; Cinnamon et al., 1999; Gros et al., 2004; Huang and Christ, 2000; Kahane et al., 1998b; Kahane et al., 2002) and to mitotic muscle progenitors (Ben-Yair and Kalcheim, 2005; Gros et al., 2005; Kahane et al., 2001; Kassar-Duchosoy et al., 2005; Relaix et al., 2005), it is not the source of the myotomal founder cells.

The earliest muscle progenitors, termed 'myotomal pioneers', arise along the medial portion of the epithelial somite (Kahane et al., 1998a), where many of them are already post-mitotic and express *MyoD*, *Myf5* and desmin. Upon dissociation, these progenitors bend underneath the forming dorsomedial lip (DML) of the DM, become mesenchymal and engage in a typical directional pattern of migration towards the rostral pole of each somite. This process is then followed by a rostral-to-caudal (R-C) and medial-to-lateral (M-L) order of fiber differentiation (Kahane et al., 2002; Kalcheim et al., 1999). Whereas medial pioneers encompass the entire M-L extent of cervical and limb-level segments, at flank regions they are complemented laterally by a population of myoblasts emerging from the lateral epithelial somite. In addition to being the first skeletal muscle cells in the embryonic somite, a recent study showed that in the absence of medial pioneers, the whole myotome is mispatterned (Kahane et al., 2007). Hence, the significance of myotomal pioneers resides in their capacity to organize further somitic waves that contribute to the developing muscle. Despite our knowledge of their cellular dynamics, the molecular mechanisms directing their unique rostralward migration and differentiation are unknown.

The Roundabout (Robo) receptor and its ligand Slit were first identified in *Drosophila* as guidance molecules for CNS axons (Kidd et al., 1998) and for muscle progenitors (Kidd et al., 1999; Kramer et al., 2001). Their vertebrate homologs play distinct roles across multiple systems (Brose and Tessier-Lavigne, 2000; Legg et al., 2008; Shiau et al., 2008; Wang et al., 2003). Robo receptors are single-pass transmembrane receptors. Robos 1-3 are mainly expressed in the nervous system (Morlot et al., 2007; Wong et al., 2001), whereas Robo 4 is specific to endothelium (Shibata et al., 2008). Slits 1-3 are multidomain leucine-rich repeat (LRR) molecules. Slit-Robo interactions are mediated by the second LRR domain of Slits and the two N-terminal Ig domains of Robos (Morlot et al., 2007). Robo members regulate Rho GTPases to affect cell motility and axonal guidance (Patel and Van Vactor, 2002). Whereas attraction is primarily mediated by Cdc42 and Rac, repulsion is executed through Rho GTPases, in particular RhoA (Dickson, 2001; Kozma et al., 1997). RhoA signals through Rock1 to enhance actomyosin contractility. It has been implicated in myosin activation and retraction of the back of the cell (Ridley, 2004; Wong et al., 2006), and has also been found to be active at the leading edge during migration (Kardash et al., 2010; Kurokawa et al., 2005; Pertz et al., 2006).

The present study is the first to document that regulation of directional migration and differentiation of pioneer myoblasts is intrinsic to the somite. In search for somite-derived signals, we found that *Robo2* is expressed by pioneer myoblasts already at the epithelial stage whereas *Slit1* is present in the DM and is abundant in the caudal half of the dissociating Scl. Loss of Robo2 function impaired the caudorostral migration of pioneers as well as myofiber formation. Similar results were obtained when Scl-derived, but not DM-derived Slit1, was abrogated. Loss of RhoA activity phenocopied the above effects and activation of endogenous Rho partially rescued the normal phenotype in pioneers lacking Robo2 activity. In all cases, myogenic specification was unaffected. By

Department of Medical Neurobiology, IMRIC and ELSC, Hebrew University-Hadassah Medical School, Jerusalem 91120–P.O.Box 12272, Israel.

*Author for correspondence (kalcheim@cc.huji.ac.il)

Accepted 27 April 2011

contrast, expression of desmin, the earliest myotomal intermediate filament protein (Bar et al., 2004), but not of myosin, was dramatically affected suggesting that Robo and Slit, through RhoA, regulate specific cytoskeletal properties. Taken together, we propose that the caudal Scl, via Slit1, acts as a negative guidance cue to direct overlying Robo2-expressing pioneer myoblasts towards the rostral domain of each segment. Slit1-Robo2 signaling also mediates their subsequent differentiation into properly aligned muscle fibers.

MATERIALS AND METHODS

Embryos

Fertile chick (*Gallus gallus*) and Japanese quail (*Coturnix coturnix Japonica*) eggs were from commercial sources (Moshav Orot and Moshav Mata).

Somite grafts

Isotopic and isochronic grafts of inverted epithelial somites were performed both before and after the onset of *MyoD* or *Myf5* expression in the medial domain; embryos were used at 16-18 or 25-27 somite stages (ss), respectively. A fragment containing the three most recently formed somites was surgically removed (Goldstein and Kalcheim, 1992). Then, somites from the left side of the donor embryo were inverted in the R-C direction and grafted into the right side of recipients from which the equivalent segments were removed in advance. Similarly, left stripes of somites were implanted into the right side of host embryos without rotation to achieve a M-L inversion.

Expression vectors, RNAi constructs and electroporation

DNA plasmids pCAGGS-GFP and YFP-C1-Lyn (from T. Meyer, Stanford University) served as controls. Rb2dN-GFP and Slit1-GFP were from S. Guthrie (Hammond et al., 2005). Dominant-negative RhoB and RhoA lacking GTPase activity (N19-RhoA and N19-RhoB) were from G. Prendergast (Adini et al., 2003). Dominant-negative MyoD consisted of the basic helix-loop-helix (bHLH) domain of mouse MyoD fused to the engrailed repressor domain [MyoD (bHLH)-enR]; E12 (bHLH)-enR served as control (Steinbach et al., 1998). MyoD and Myf5 expression vectors were from D. Duprez (Universite Pierre et Marie Curie, Paris). The following RFP-tagged RNAi constructs were employed: RNAi to cSlit1, RNAi to cRobo2 or RNAi to GFP (Shiau et al., 2008). DNA (3-5 mg/ml) was microinjected into the three or four recently formed somites. A square wave electroporator (BTX, San Diego, CA, USA) was used to deliver two pulses of current at 15 V for 10 milliseconds to the medial somite and one pulse at 9 V for 10 milliseconds to the ventral or dorsal somite (prospective Scl or DM, respectively).

Grafting of pluronic gel

Pluronic F-127 gel was prepared as described (Groysman et al., 2008) and mixed with 100 μg/ml lysophosphatidic acid (LPA). Small pieces of control or LPA-containing gels were placed dorsal to the embryo at the level of epithelial somites, and replaced every 4-5 hours, for a total of 14 hours.

Tissue processing, immunocytochemistry and in situ hybridization

Embryos were fixed with 4% formaldehyde and either wax embedded and sectioned at 10 μm, or observed as whole-mount preparations following evisceration and flattening.

Antibodies used were: anti-Desmin and anti-GFP (Molecular Probes), Myf5 (Yablonka-Reuveni and Paterson, 2001), N-cadherin (Shoval et al., 2007), p27 (Kahane et al., 2007), anti-caspase 3 (Cell Signaling) and anti-sarcomeric myosin [MF20 (Developmental Studies Hybridoma Bank)]. Secondary antibodies coupled either to Cy2, Cy3 or Cy5 were used (Jackson ImmunoResearch). In situ hybridization was performed as described (Cinnamon et al., 2001) using probes for chick *MyoD* and *Myf5* (from D. Duprez); *Robo1*, *Robo2*, *Slit1*, *Slit2* and *Slit3* (from Ed Laufer, Columbia University, NY); and *desmin*, *rhoA*, *rhoB* and *Wnt11* (from the BBSRC ChickEST Database) (Boardman et al., 2002). Nuclei were visualized with Hoechst.

Data analysis

The number of desmin-expressing mesenchymal progenitors, elongating cells or unit-length myofibers was analyzed on whole-mount preparations. Confocal sections that encompassed the entire thickness of the myotome were monitored using 40× or 60× objectives at 0.5-0.65 μm increments through the *z*-axis. In each optical section constituting part of a transfected cell, green and red channels were systematically compared to assess expression of desmin or myosin proteins. The dorsoventral analysis was complemented by performing transverse projections of the images. Results represent the mean percentage ± s.e.m. of total GFP-labeled cells in 10-20 embryos per treatment. Mesenchymal cells were defined by their typical fibroblastic shape, elongating cells were defined when their long axis was at least threefold the length of the short axis.

Whole-mounts and sections were photographed using a DP70 (Olympus) cooled CCD digital camera mounted on a BX51 microscope (Olympus) with Uplan FL-N 10×/0.30, 20×/0.5 and 40×/0.75 dry objectives (Olympus) at room temperature, using DP controller v1.2.1.108 acquisition software (Olympus). Confocal scanning was carried out using an Olympus Fluoview FV1000 with 10×/0.4 20×/0.75 40×/0.9 dry and 60×/1.35 oil objectives, software version 1.7c. For figure preparation, images were exported into Photoshop CS2 (Adobe). If necessary, the brightness and contrast were adjusted to the entire image and images were cropped without color correction adjustments or γ adjustments.

Statistical analysis

Significance of results was determined using the Mann-Whitney non-parametric test or Fisher's exact test. Control and two experimental groups were also compared using the Kruskal-Wallis non-parametric test, followed by the Mann-Whitney test, for pairwise comparisons, with Bonferroni correction of the significance level. All tests applied were two-tailed, and a *P*-value of 0.05 or less was considered significant.

RESULTS

Rostro-caudal (R-C) or medio-lateral (M-L) somite inversions reveal that the directionality of pioneer myotome development is intrinsic to the somite

To investigate whether the caudal-to-rostral migration of pioneer myoblasts is an intrinsic property of the somite or is controlled by surrounding tissues, quail or chick epithelial somites were grafted into chick hosts so that either the R-C or the M-L axes were independently switched. This was performed both before as well as after initial expression of *MyoD*, *Myf5* and desmin. Chimeras were fixed at a stage when an overall triangular shape of pioneer cells was apparent (Figs 1, 2). As previously shown, this pattern is accounted for by pioneers differentiating in both R-C and M-L directions, with medially located fibers and the lateral-most cells still mesenchymal and preferentially restricted to the rostral half of segments (Kahane et al., 2002).

Rostro-caudal somite inversions

A stripe of three somites that already expressed desmin was removed from the left side of 25ss embryos and grafted into the right side of equivalent hosts after R-C inversion (Fig. 1A-B′, asterisks). In all chimeras, the grafted somites showed an inverted pattern of fiber elongation, demonstrating that the pioneer myoblasts had migrated and were undergoing differentiation according to their original polarity (*n*=13, Fig. 1A-B′). When the same procedure was performed at 16-18ss, prior to the onset of *MyoD*, *Myf5* or desmin expression (Fig. 1C-D′, asterisks), a similar, inverted pattern of pioneer development was observed (Fig. 1C,D″, asterisks) when compared with the contralateral side (*n*=10, arrows). These results suggest that the directional R-C behavior of pioneer myoblasts is determined early during somite formation.

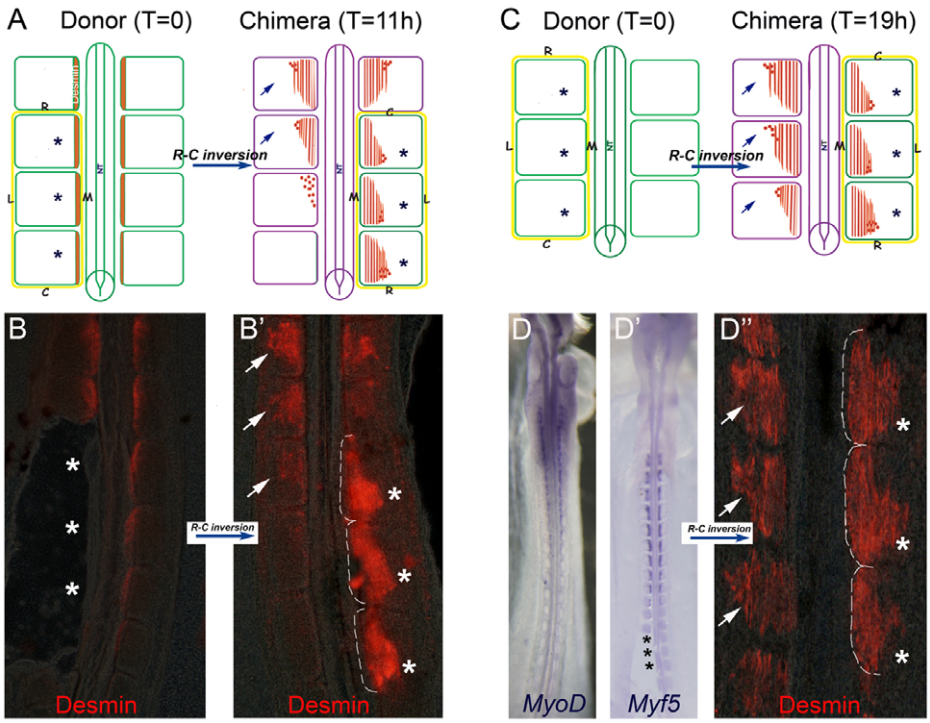

Fig. 1. Rostrocaudal somite inversions reveal that the directional pattern of pioneer myotome development is intrinsic to the somite. (**A-B′**) Three epithelial somites expressing desmin (asterisks and yellow frame in A) were removed from the left side of 25ss quail embryos and grafted into the right side of equivalent chick hosts after rostral-to-caudal (R-C) inversion without affecting the medial-to-lateral (M-L) axis. Note the inverted pattern of fiber elongation in the chimera (asterisks in B′, segments demarcated by dashed lines) compared with control somites at T=11 hours (arrows in A and B′). Comparison is made with more mature somites because of a delay in desmin expression in chick versus quail. (**C-D″**) The same procedure performed at 18ss prior to the onset of *MyoD* (D), *Myf5* (D′) or desmin (D″) expression. Asterisks in D′ illustrate the level of somite excision. (D″) Note that 19 hours later an inverted pattern of pioneer development (asterisks) compared with arrows in control side. Dashed lines delineate segment boundaries. C, caudal; L, lateral; M, medial; NT, neural tube; R, rostral.

Medio-lateral somite inversions

A stripe of three desmin-positive epithelial somites was removed from the left side of 25ss embryos (Fig. 2A, asterisk in 2B) and grafted into the right side of equivalent hosts, thus achieving a M-L inversion without altering the R-C axis (Fig. 2A, asterisk in 2B′). In all chimeras, the grafted somites showed an inverted pattern of fiber elongation with long fibers located laterally and short fibers/mesenchymal cells pointing medially (*n*=19, Fig. 2A,B′); this pattern suggests that pioneers kept their original M-L polarity. When performed on young somites before expression of myogenic genes, a de novo induction of desmin+ progenitors was observed along the medial edge adjacent to the neural tube, consistent with the notion that axial structures have a role in early myogenesis (see Discussion). However, in 10/12 embryos, only few original medial pioneers appeared laterally (not shown), probably because they failed to upregulate myogenic markers in the absence of axial signals and/or were deprived of survival signals and died. Regardless of the exact mechanism, analysis of the migratory behavior of medial pioneers following M-L inversions at a young stage was not achievable. To control for possible effects of microsurgery, similar somite replacements that kept their original R-C (*n*=4) or M-L (*n*=3) orientations were performed, which resulted in a normal pattern of pioneer behavior (not shown).

Collectively, R-C and M-L somite inversions show that the rostralward migration of mesenchymal pioneers and subsequent M-L expansion of the nascent fibers are directed by cues intrinsic to the somite.

Slit1-Robo2 signaling mediates migration and differentiation of pioneer myoblasts

Next, we searched for somite-derived factors for which expression differs along the R-C domain. Genes differentially expressed in rostral (R) versus caudal (C) domains of the Scl were shown to determine the segmental patterning of migrating neural crest precursors, as well as of peripheral axons, via repellent mechanisms (Kalcheim, 2000; Krull, 2001; Le Douarin and Kalcheim, 1999; Roffers-Agarwal and Gammill, 2009; Vermeren et al., 2000).

Robo2 is expressed in medial pioneer myoblasts and Slit1 in the caudal Scl and DM

Robo2 mRNA was already expressed in early pioneer cells that constitute the medial epithelial somite (Fig. 3A,D, asterisk in 3G), then in the developing primary myotome at a stage previously shown to correspond to caudal-to-rostral (C-R) migration (Fig. 3A,C,F) (see Kahane et al., 1998a; Kahane et al., 2002) and in fully differentiated fibers (Fig. 3A,B,E). By contrast, *Robo1* and *Robo3* were not transcribed in the medial somite (not shown).

Slit1 mRNA was preferentially transcribed in the C domain compared with the R domain of the ventral epithelial somite and nascent Scl; in addition, it was homogeneously expressed in the DM (Fig. 3H,J-L). Upon full dissociation into DM and Scl, *Slit1* was downregulated in both primordia (Fig. 3H-I′). Only later (E3.5-4) did *Slit1* appear in the DML and ventrolateral lip (VLL) after dissociation of the DM sheet (not shown). *Slit2* and *Slit3* were restricted to the dorsal neural tube (NT) and notochord, or notochord only, respectively (not shown). The specific expression of *Robo2* to pioneer myoblasts and of *Slit1* to the Scl and DM, motivated us to examine their function in development of the pioneer wave.

Loss of directional migration and abnormal morphogenesis of pioneer myoblasts lacking Robo2 gene activity

Membrane-tethered GFP (YFP-C1-Lyn) or Rb2dN-GFP, a truncated version of Robo2 lacking the cytoplasmic domain, were electroporated into medial pioneers at the epithelial somite stage (Fig. 4A). Sixteen hours later, control YFP-C1-Lyn+ cells had organized into a typical triangular shape composed medially of elongating fibers and laterally of mesenchymal cells primarily confined to the R domain (*n*=186 cells counted in 12 segments

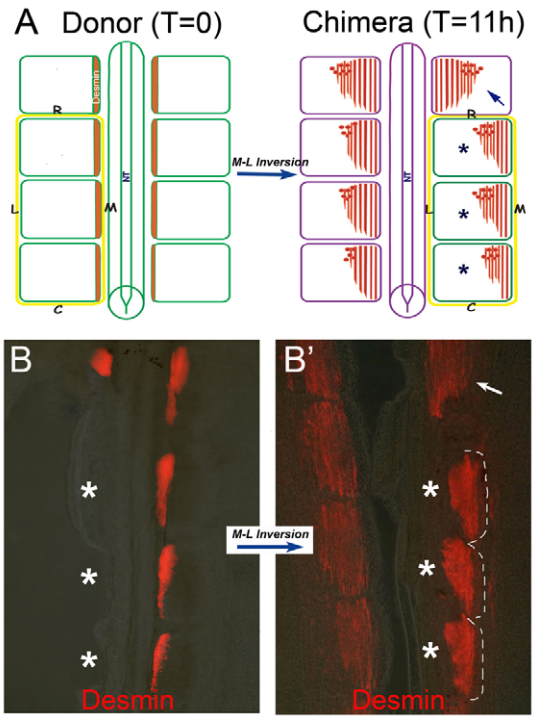

Fig. 2. Mediolateral somite inversions reveal that the directional pattern of pioneer myotome development is intrinsic to the somite. (**A**,**B**) Three epithelial somites (yellow frame in A and asterisks) that express desmin (see contralateral somites) were removed from the left side of 25ss quail embryos and grafted into the right side of equivalent chick hosts so that the M and L sides are inverted without altering the rostral-to-caudal (R-C) axis. (**B′**) Note the inverted pattern of fiber elongation in the chimera (compare asterisks with upper arrow, see also A, right panel) with long fibers laterally located and short fibers/mesenchymal cells pointing medially. Dashed lines delineate segment boundaries. C, caudal; L, lateral; M, medial; NT, neural tube; R, rostral.

from a total of five embryos, Fig. 4B,D,J-L). In contrast with the controls, the majority of Rb2dN-GFP+ cells remained mesenchymal (Fig. 4E,F,J, $P<0.001$) and distributed homogeneously along the R-C extent of the transfected segments (Fig. 4C,K, $P<0.001$). Those which succeeded in elongating (13% versus 66% in controls, $P<0.001$) did so aberrantly from either the R lip, the C lip or from elsewhere along the segment compared with control cells that coherently elongated in a R-C direction ($n=202$ cells in 18 segments/ten embryos, Fig. 4F,L).

When fixed 24 hours after electroporation, 96% of control GFP+ cells had already differentiated into typical long and thin unit-length muscle fibers compared with only 37% in Rb2dN-GFP-transfected cells (see Fig. S1 in the supplementary material, $P<0.006$). The Rb2dN-GFP+ cells that elongated, did so aberrantly from different origins ($n=68$ cells in 19 segments/seven embryos), were abnormally wide in shape and exhibited irregular membrane protrusions that were not observed in wild-type myofibers (see Fig. S1B-D in the supplementary material).

Differential effects of Rb2dN on expression of desmin, myosin and myogenic genes

The vast majority of control pioneers co-expressed desmin immunoreactivity (97%), a marker that first appears at the epithelial stage. In striking contrast, only 8% and 23% of Rb2dN-GFP-treated progenitors did so when monitored 16 and 24 hours post-transfection, respectively ($P<0.001$ for both stages, Fig. 4G-J and see Fig. S1 in the supplementary material). This dramatic reduction of desmin protein was not accounted for by cell death, as few, if any, caspase-3 or TUNEL-positive cells were apparent in control or treated myotomes (see Fig. S1E,F in the supplementary material; not shown). Furthermore, in spite of interfering with the onset of desmin protein expression, Rb2dN-GFP did not inhibit *desmin* transcription ($n=12$, see Fig. S2A-B′ in the supplementary material). Next, we examined whether Robo2 activity is required for steady desmin expression. To this end, Rb2dN-GFP was transfected into epithelial pioneers at a later stage (25ss) following initial appearance of desmin protein. Under these conditions, desmin immunoreactivity was preserved (not shown) suggesting that Robo2 is necessary for initial expression of desmin protein but not for its maintenance. Because desmin lies downstream of *Myf5* and *MyoD*, we examined whether loss of Robo2 affects the latter. Early transcription of either *MyoD* ($n=20$) or *Myf5* ($n=6$), or expression of Myf5 immunoreactive protein ($n=2$) were unaffected (see Fig.S2C-H′ in the supplementary material). As part of the myogenic program following *MyoD* and *Myf5* expression, pioneer myoblasts become postmitotic (Kahane et al., 1998a). Loss of Robo2 activity did not prevent them from exiting the cell cycle normally (not shown) or from expressing p27 ($n=5$, see Fig. S2I-J′ in the supplementary material). Furthermore, epithelial pioneers were shown to express N-cadherin yet lose it upon dissociation and migration (Cinnamon et al., 2006); loss of Robo2 function did not alter the normal dynamics of N-cadherin ($n=5$, see Fig. S2K-L′ in the supplementary material and not shown) indicating that, in this context, Robo might act via cadherins other than N-cadherin (Emerson and Van Vactor, 2002; Rhee et al., 2002).

Next, we asked whether Robo2 specifically affects desmin protein. To this end, we monitored expression of myosin with the MF20 antibody that labels both fast and slow myosin heavy chains. Fig. S3A in the supplementary material shows that in normal embryos, although desmin immunoreactivity is already detected in the medial epithelial somites (see also Fig. 1B and Fig. 2B), myosin immunoreactivity becomes first apparent in somite 12 of 25ss embryos where it stains only a subset of differentiating myoblasts (see Fig. S3B,B3,B4 in the supplementary material). Hence, because of the relatively late onset of myosin expression (Sacks et al., 2003), the early behavior of pioneer myoblasts (epithelial stage and C-R migration) can only be monitored using desmin as a marker. Therefore, to monitor effects on myosin, embryos were electroporated and fixed at a differentiation stage at which full-length myofibers were present in control segments (see Fig. S3C-C‴ in the supplementary material). As described above, Rb2dN-GFP-transfected cells were abnormal in shape and failed to generate normally elongated fibers (see Fig. S1 and Fig. S3D-D″ in the supplementary material). Nevertheless, myosin expression was not affected (see Fig. S3C-F in the supplementary material). A faithful quantification of the proportion of myosin-expressing out of total transfected cells was, however, not possible as this protein was expressed by only a subset of myotomal cells under both experimental conditions. Hence, Robo2 signaling specifically influences the onset of desmin expression without affecting the later appearance of myosin.

To assess further the specificity of the Robo2 phenotype, we used RNAi-mediated knockdown (Shiau et al., 2008). Robo2-RNAi phenocopied the effects of truncated Robo2; it perturbed the normal generation of unit-length fibers and reduced expression of desmin, but had no effect on initial myoblast specification as monitored by transcription of *Myf5* ($n=4$ and $n=7$ for control-RNAi and Robo2-RNAi, respectively, see Fig. S4 in the supplementary material).

Fig. 3. *Robo2* is expressed in medial pioneer myoblasts and *Slit1* in the caudal sclerotome (Scl) and dermomyotome (DM). (**A-G**) Pioneer myoblasts are enriched with *Robo2* mRNA. Initial expression is in the medial epithelial somite (D,G), then in delaminating progenitors (C,F) and in cells that localize to the rostral domain of the somite (arrows in C); subsequently, *Robo2* is in recently formed myofibers (B,E). (**H-L**) *Slit1* is abundant in the caudal (asterisks in J′,K′,L) compared with the rostral (J,K,L) halves of the nascent Scl. Upon full dissociation, *Slit1* is downregulated in both Scl and DM (I,I′). Note lateral expression of *Slit1* in the mesonephric tubules. In L, rostral is to the top. Embryos are 30 somites old. C, caudal; DS, dissociating somite; L, lateral; M, medial; NT, neural tube; R, rostral. Scale bar: 280 μm in E-G; 200 μm in I-K′; 150 μm in L.

Together, these data suggest that Robo2 activity is necessary for the normal directional migration of pioneer myoblasts and for the formation of fibers with a normal morphology.

MyoD and Myf5 are necessary and sufficient for cRobo2 expression

Next, we examined whether myogenic genes upregulate *cRobo2* transcription. To this end, MyoD and Myf5 were misexpressed in the prospective DM, a domain that is normally negative for *Robo2* except for its medial-most domain. Sixteen hours later, *Robo2* mRNA was upregulated in DM cells overexpressing MyoD and Myf5, compared with GFP controls (n=9, 5, 5, respectively; see Fig. S5A-C″ in the supplementary material).

Reciprocally, to examine whether myogenic genes are necessary for *cRobo2* expression in pioneers, we transfected MyoD (bHLH)-enR into medial epithelial somites. As control, we electroporated E12 (bHLH)-enR, in which the basic region was replaced by the corresponding sequence of the non-myogenic dimerization partner of MyoD. Whereas MyoD (bHLH)-enR inhibited both MyoD as well as Myf5-induced myogenesis in chick somites, E12 (bHLH)-enR had no effect, confirming their specificity (not shown). Consistently, a dramatic decrease in *cRobo2* expression was detected in pioneer progenitors expressing MyoD (bHLH)-enR whereas no effect was observed in controls (n=7 and n=5, see Fig. S5D-E″ in the supplementary material). Together, these data suggest that Robo2 acts downstream of myogenic genes to affect the assembly of the desmin-containing cytoskeleton.

RNAi to Scl-derived Slit1 phenocopies the effects of loss of Robo2 function on pioneer myoblasts

The preceding grafting experiments (Figs 1 and 2) suggested that the cues for directional behavior of pioneer myoblasts are somite-intrinsic. *Slit1* is transiently expressed in DM and caudal Scl. Consequently, we inhibited Slit1 function with plasmid-based RNAi previously used in the nervous system (Shiau et al., 2008). Concomitantly, to identify the origin of active Slit1, we separately abrogated its activity in either the Scl or the DM by electroporating labeled RNAi to Slit1 or control RNAi-RFP either to the ventral or dorsal somite.

Confocal analysis revealed normal desmin+, Myf5+ fibers when control RNAi-RFP (GFP-RNAi) was transfected into the Scl (n=53 somites/15 embryos, Fig. 5A,A′,C,H). Furthermore, electroporation of the DM with GFP-RNAi or Slit1-RNAi did not interfere either with normal pioneer development (n=13 somites/four embryos, Fig. 5G,G′ and not shown). By contrast, most myoblasts overlying the Scls that received Slit1-RNAi were devoid of, or exhibited reduced, desmin immunolabeling (n=95 somites/23 embryos, Fig. 5B,B′, P<0.001). However, they expressed *desmin* mRNA (Fig. 5D,E) and Myf5 (Fig. 5I) (n=10 and n=9, respectively). Expression of *desmin* mRNA revealed that cells were disorganized and, instead of generating fibers, remained mesenchymal (Fig. 5D,E), similar to pioneers depleted of Robo2 function. In an attempt to rescue the above phenotypes, we co-electroporated Slit1-RNAi and human Slit1-GFP, which is not blocked by chick RNAi. In nine of 11 such embryos (36/41 segments), we observed the presence of elongated, desmin+ fibers that resembled the control situation (Fig. 5F,F′, P<0.002), further confirming the specificity of the observed effects. Hence, cross talk between Scl-derived Slit1 and Robo2-carrying pioneers might mediate the early patterning of the avian myotome.

RhoA operates downstream of Slit1-Robo2 to promote development of pioneer fibers

Slit- and Robo-mediated axonal repulsion was shown to stimulate RhoA activation (Patel and Van Vactor, 2002; Wong et al., 2001). Because Slit1- and Robo2-dependent migration of pioneers also consists of an initial phase of myoblast ‘repulsion’ from the C domain of each segment towards the R domain, we examined whether Rho GTPases are involved.

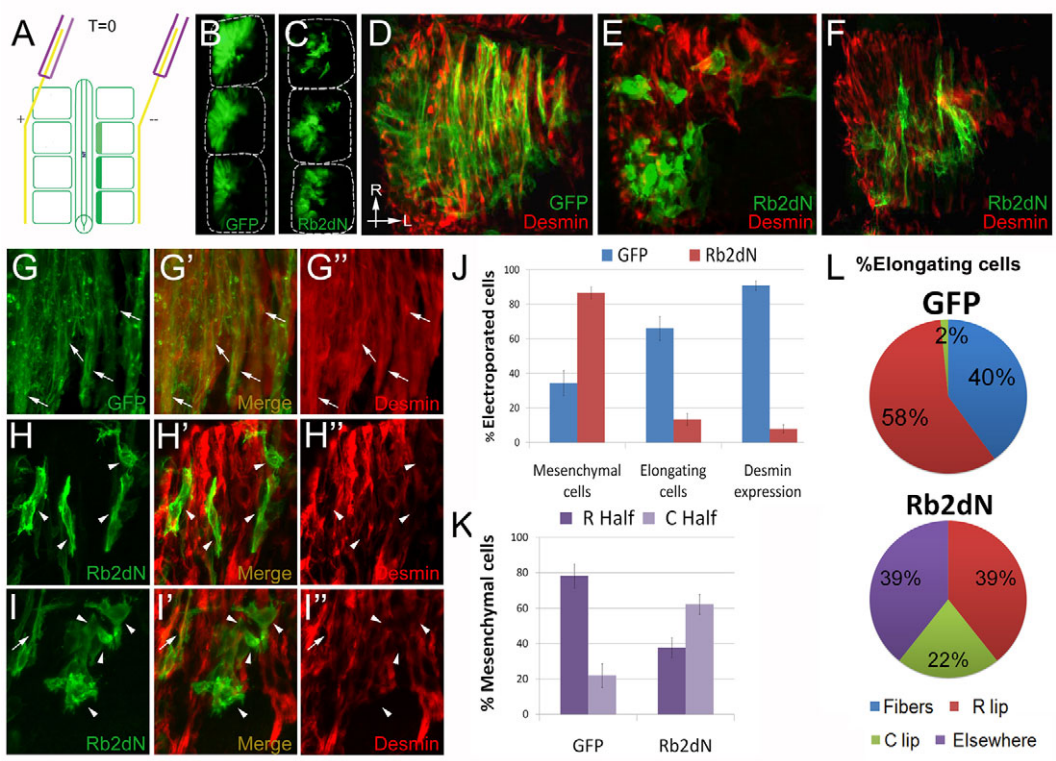

Fig. 4. Loss of rostrocaudal polarity and abnormal morphogenesis of pioneer myoblasts lacking Robo2 activity. (**A**) Scheme of electroporation into pioneers. DNA was injected into the lumen of epithelial somites of 16-18ss embryos and current was directed to the contralateral side (+ pole). (**B**,**C**) Dorsal views 16 hours later to show in control-GFP-transfected segments (B) the triangular shape accounted for by a higher number of labeled pioneers in the rostral somite halves. By contrast, Rb2dN/GFP+ cells distribute randomly along the rostral-to-caudal (R-C) extent of segments (C). (**D-F**) Confocal images of individual segments showing normal fiber development of control pioneers that co-express desmin (D). (E,F) Rb2dN/GFP+ cells largely fail to elongate, and are randomly distributed with a preference for the caudal somite domain. (**G-I″**) High magnifications of dorsal views to show control GFP+ cells co-expressing desmin (arrows in G-G″) whereas most Rb2dN/GFP+ cells lack desmin immunoreactivity (H-H″ and I-I″, arrowheads). Arrow in I-I″ shows a double-positive cell. (**J**) Quantification of the distribution of pioneers 17 hours after transfection as mesenchymal or elongating cells and of the proportion of desmin-expressing cells. Error bars represent s.e.m. (**K**) Quantification of the distribution of mesenchymal pioneers to the rostral (R) versus caudal (C) somite halves. Error bars represent s.e.m. (**L**) Quantification of the distribution of elongating pioneers from various origins. Statistical analysis used the Mann-Whitney non-parametric test.

A low level of *RhoA* transcripts was first detected in pioneer myoblasts residing in the medial epithelial somite. *RhoA* signal intensified upon pioneer delamination and migration and persisted throughout differentiation (see Fig. S6A-D in the supplementary material). By contrast, *RhoB* mRNA was absent during early phases of pioneer development and began to be transcribed in differentiated fibers with transcripts preferentially localized around the centrally located nuclei (see Fig. S6E-I in the supplementary material).

Next, we monitored the effects of inhibiting either RhoA or RhoB, the latter used as control because of its late onset compared with RhoA. Inhibition was achieved by overexpression of N19-RhoA or N19-RhoB, which lack GTPase activity (Adini et al., 2003). These constructs were shown to have differential effects on delamination of neural crest cells (Groysman et al., 2008). Control GFP or N19-RhoB-electroporated segments exhibited a characteristic pattern composed of desmin+ medial fibers and lateral elongating cells (Fig. 6A-B‴,D-F; n=330 cells/19 segments/eight embryos and n=42 cells/four segments/three embryos in control and N19-RhoB, respectively). By contrast, most N19-RhoA-transfected cells remained mesenchymal and many of them failed to migrate rostralward (P<0.001) and exhibited reduced desmin expression (Fig. 6C-F, n=387 cells/18 segments/seven embryos, P<0.001 for all parameters compared in Fig. 6D). Transfected cells that succeeded to elongate did so from different origins (R lip, C lip, elsewhere) when compared with control or N19-RhoB that exhibited, as expected, directional fiber differentiation from R to C (Fig. 6F). In summary, loss of RhoA function phenocopied the effects of loss of Robo2 function.

Activation of endogenous Rho signaling with lysophosphatidic acid (LPA) partially rescues loss of Robo2 activity

To assess whether RhoA operates downstream of Robo in myotomal pioneers, we examined whether Rho activation can rescue the phenotype caused by loss of Robo2. First, we electroporated full-length and constitutively active forms of RhoA or RhoB to medial pioneers. Both GTPases caused death of the transfected cells as previously observed in the neural tube (Groysman et al., 2008), precluding further analysis. To circumvent this limitation, endogenous Rho activity was stimulated by LPA. LPA is a bioactive phospholipid that signals through G-protein-coupled receptors and promotes cytoskeletal reorganization through activation of the Rho pathway (Li et al., 2003; Ren et al., 1999; Ridley and Hall, 1992; Weiner et al., 2001). Small pieces of control

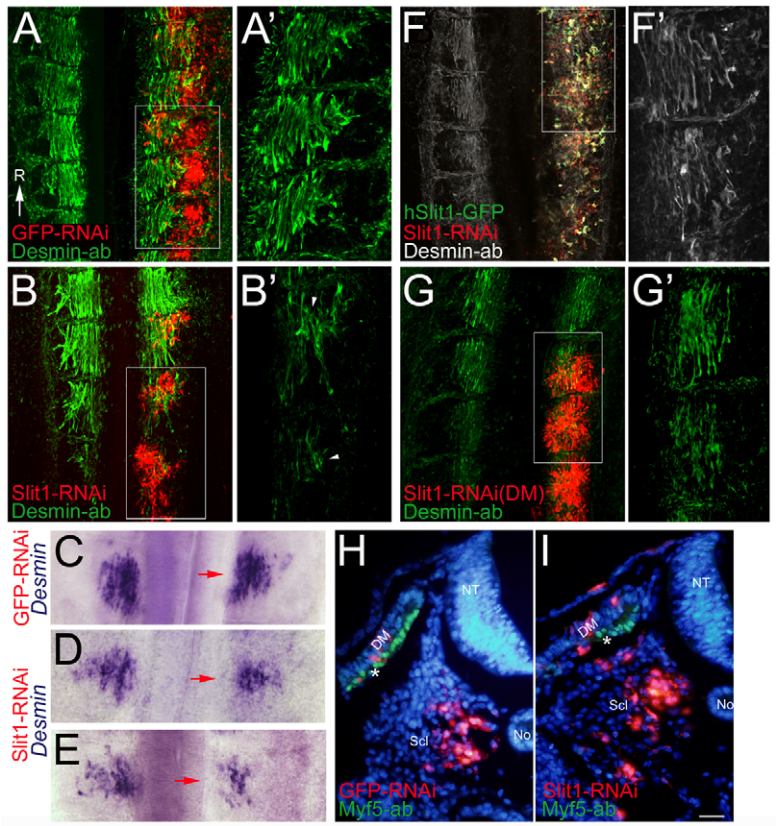

Fig. 5. RNAi to sclerotome (Scl)-derived Slit1 phenocopies the effects of loss of Robo2 function on pioneer myoblasts. (**A-I**) (A,A′,C,H) GFP-RNAi-RFP; (B,B′,D-G′,I) Slit1-RNAi-RFP. For expression in the dermomyotome (DM), electroporation was ventrodorsal (G,G′) and for Scl expression was dorsoventral (all other panels). Electroporations were at 16-18ss. (A,A′) Integrated confocal images show normal desmin+ fibers (green) overlying the control RNAi-transfected Scls (red). By contrast, cells overlying the Scls that received Slit1-RNAi show significantly reduced desmin protein and irregular morphology (B,B′, arrowheads). (C-E) Dorsal view of whole mount in situ hybridization for *desmin* after control-RNAi (C) or Slit1-RNAi (D,E). In both cases, transfected cells expressed *desmin* mRNA (red arrows). The large size of fibers in controls account for the robust staining observed, whereas Slit1-RNAi-treated pioneers remained as small and disorganized mesenchymal progenitors. (F,F′) Dorsal view of somites after co-electroporation of Slit1-RNAi (red) and human Slit1-GFP (green) showing rescue of desmin+ myofibers (gray, magnification in F′). (G,G′) Integrated confocal images showing normal desmin+ fibers (green) ventral to the Slit1-RNAi transfected DMs (note their typical epithelial appearance, red). (H,I) Transverse sections of somites that received control-RNAi (H) or Slit1-RNAi (I) showing Myf5 protein (green) in myotomes (asterisks). No, notochord, NT, neural tube. Scale bar: 90 μm in H,I.

gel or LPA-containing pluronic gel were placed dorsal to the embryo in ovo, embryos were fixed 14 hours later and were analyzed for desmin expression, cell migration and differentiation.

Seventy-three percent of labeled pioneer cells were present in the R domain of somites that received control or LPA-containing gels (Fig. 7A-B′,F,G; n=199 cells/15 segments/seven embryos and 157 cells/16 segments/nine embryos, respectively). By contrast, only 42% of Rb2dN+/control gel-treated pioneers were present in the R domain (Fig. 7C,C′,F,G; n=74 cells/16 segments/seven embryos, P<0.001). Treatment with LPA of pioneers that received Rb2dN enhanced the proportion of rostrally located pioneers to 63% (Fig. 7D,D′,F; n=159 cells/20 segments/ten embryos, P<0.001). In addition, treatment with LPA stimulated expression of desmin immunoreactivity (50% of Rb2dN+ pioneers) compared with 15% in Rb2dN+/control gel and 95-98% in control GFP/control gel (Fig. 7A″-D″,F, P<0.001 for all comparisons). Nevertheless, LPA did not significantly enhance the percentage of elongating cells in Rb2dN-transfected cells (Fig. 7F). Hence, activation of endogenous Rho partially rescued the effects of loss of Robo2 function both on desmin expression and pioneer migration towards the R domain, but could not completely reverse the phenotype. Altogether, our results show that RhoA mediates the repulsive effect of Slit1 and Robo2 on selected aspects of pioneer myoblast development.

DISCUSSION

Lineage tracing studies identified the existence and dynamic behavior of distinct pioneer myoblasts in the avian embryo (Kahane et al., 1998a), and inhibition of their specification demonstrated their pivotal role in myotomal patterning (Kahane et al., 2007). However, the molecular mechanisms underlying pioneer development remained unknown. Here, we show that their unique directional migration and differentiation is regulated by somitic cues, and identify Robo2 and Scl-derived Slit1 as mediators of the these processes through RhoA signaling and desmin protein expression.

Studies on avian mesoderm patterning showed that specification of individual somites along their R-C extent is a somite-intrinsic property arising already prior to segmentation; by contrast, dorsoventral somite patterning, as well as the commitment of the medial somite to a myogenic fate, seem to be induced by signals from adjacent structures (Borman and Yorde, 1994; Buffinger and Stockdale, 1994; Dietrich et al., 1997; Kenny Mobbs and Thorogood, 1987; Münsterberg et al., 1995; Münsterberg and Lassar, 1995; Pownall et al., 1996; Rong et al., 1992; Stern et al., 1995; Vivarelli and Cossu, 1986) (for reviews, see Bothe et al., 2007; Christ et al., 2007; Christ and Scaal, 2008). Our results stemming from M-L somite inversions, performed prior to the onset of *MyoD* or *Myf5* expression, are consistent with the axial structures inducing the medial somite to generate pioneer myoblasts. In addition, results of R-C somite inversions show that actual patterning of the first wave of muscle progenitors, represented by an initial C-R migration of myoblasts, is subjected to somite-intrinsic polarity cues, previously described to control the R-C patterning of the somite-derived Scl. Likewise, the segmental organization of adjacent neural crest-derived peripheral ganglia, Schwann cells and nerves is also subservient to intrinsic R-C differences within the Scl that are mediated by several families of repellent molecules (see Results). These intra-Scl differences are also reflected in the generation of components of the vertebrae (Goldstein and Kalcheim, 1992). Thus, collectively, intrinsic differences between early R-C somite domains affect the patterning of virtually all local derivatives including neural as well as skeletal (muscle and vertebrae) components.

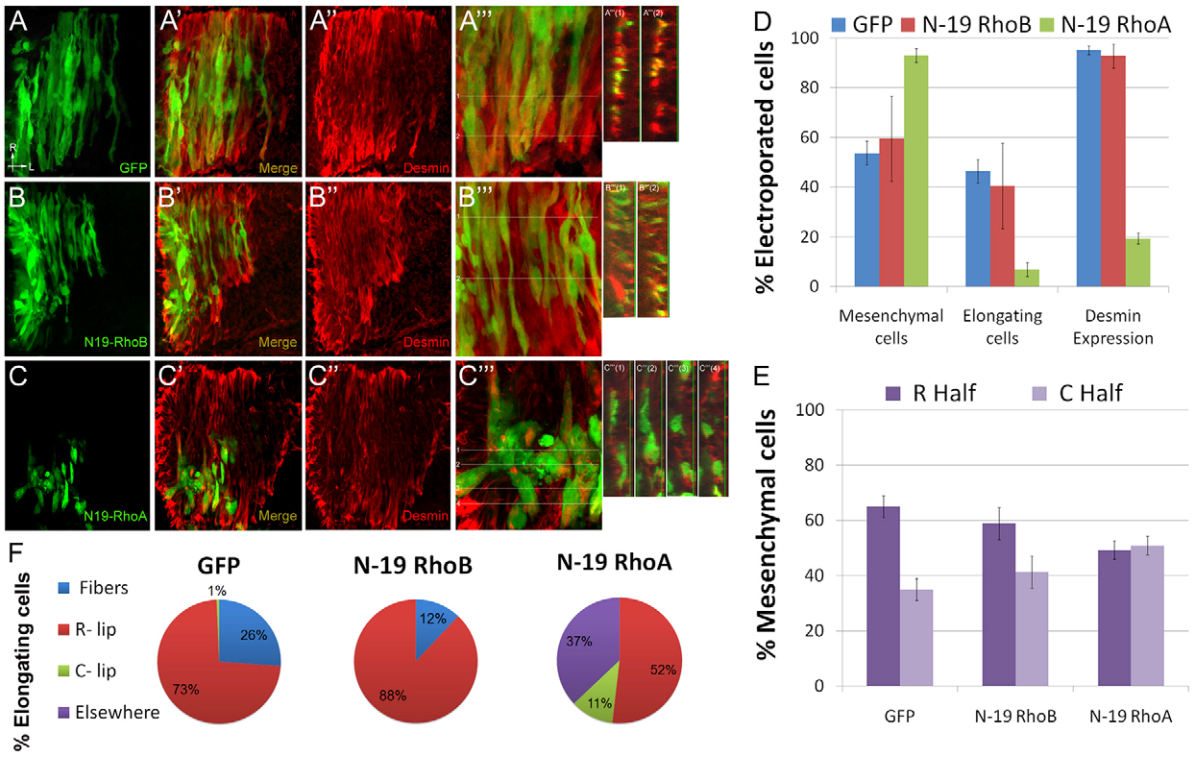

Fig. 6. Loss of RhoA activity, but not of RhoB, phenocopied the effects of loss of Robo2 function. (**A-B‴**) Dorsal views of control GFP (A-A‴), or N19-RhoB-electroporated segments (B-B‴) showing formation of normal GFP+ fibers that co-express desmin (yellow reflects the overlay of green GFP and red desmin). This is also appreciated in the transverse projections through levels 1 and 2 in A‴ and B‴, shown as [A‴ (1),A‴ (2),B‴ (1),B‴(2)]. (**C-C‴**) N19-RhoA-transfected cells remained mesenchymal, failed to migrate rostrally and most were devoid of desmin (green and red colors distinctly separated). C‴(1)-(4) represent transverse projections through levels 1-4 in panel C‴. Electroporations were at 16-18ss and embryos were fixed 16 hours later. (**D**) Quantification of the distribution of transfected pioneers as mesenchymal versus elongating cells and of the proportion of desmin-expressing cells. Error bars represent s.e.m. (**E**) Quantification of the distribution of mesenchymal pioneers in the rostral (R) versus caudal (C) somite halves. Error bars represent s.e.m. (**F**) Quantification of the distribution of elongating pioneers and of the proportion of unit-length fibers. Statistical analysis used the Kruskal-Wallis non-parametric test followed by the Mann-Whitney test for pairwise comparisons.

Once differentiated, pioneer myofibers provide a scaffold for further myotomal organization (Kahane et al., 2007). The latter is accounted for by a second wave of muscle colonization stemming from all four lips of the DM once it forms (Cinnamon et al., 2001; Cinnamon et al., 1999; Gros et al., 2004; Huang and Christ, 2000; Kahane et al., 1998b; Venters et al., 1999), including the DML (Denetclaw et al., 2001; Denetclaw et al., 1997; Ordahl et al., 2001) and VLL (Denetclaw and Ordahl, 2000). Nevertheless, we suggest that the mechanisms by which DM-derived progenitors develop differ significantly from that of pioneers. Only pioneers are likely to respond to caudal Scl-derived Slit1, which drives their rostralward migration. Subsequent to Scl maturation, at a stage corresponding to the onset of DM lip contribution to the myotome, *Slit1* is no longer expressed (see Fig. 3). This downregulation of *Slit1* might enable second wave cells to elongate in both R and C directions, contrary to the transient directional behavior of earlier pioneers. Furthermore, Wnt11 from the DML, shown to orientate elongation of myocytes derived from the DML of the DM (Gros et al., 2009), is unlikely to direct migration and/or differentiation of pioneers as detectable *Wnt11* mRNA became apparent only after pioneer myoblasts had accomplished migration, and its expression was homogeneous along the R-C extent of the lip (see Fig. S7 in the supplementary material and O.H.-B., unpublished). Furthermore, pioneer myoblasts can be distinguished from DM-derived fibers by differential electroporation to the medial versus dorsal somite domains, respectively. Labeling of the medial somite generates a triangular pattern of elongating fibers and lateral mesenchymal cells 14 hours later and fully elongated fibers by 24 hours. By this time, the DM, including the DML, has not yet contributed to myotome colonization (see Fig. S8 in the supplementary material). Consistently, pioneer myoblasts are mostly a post-mitotic (Brdu–/p27+) and finite cell population, whereas progenitors of the DML of the DM behave as a stem-like cell population. Hence, the present results add to previous lineage and molecular evidence to further support the notion that the establishment of pioneer fibers and that of subsequent DML-derived fibers are distinct and separable events (Cinnamon et al., 2006; Kahane et al., 2002).

We report that Slit1 mediates the repellent activity of the caudal Scl by acting upon Robo2-expressing pioneer myoblasts to drive rostralward migration. Similarly, *Drosophila* midline Slit acts as a long-range cue to initially repel muscle precursors away from the midline (Kidd et al., 1999). The present report is the first to document vertebrate muscle patterning through a repellent mechanism and, particularly, to demonstrate the activity of specific Slit-Robo members. In addition to an effect on R-C redistribution, we also report for the first time an effect of Robo/Slit on the generation of normal fiber morphology. It is likely that defects in migration provoked further abnormalities in myofiber development, as normal pioneers elongate from the

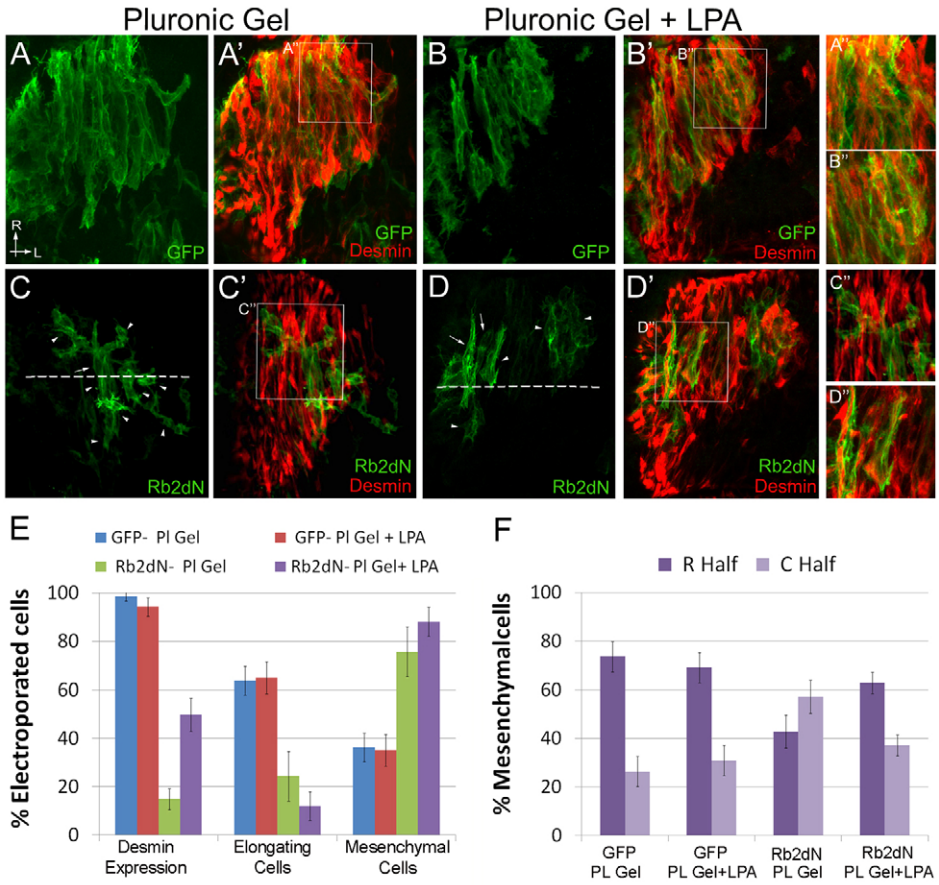

Fig. 7. Lysophosphatidic acid (LPA)-mediated activation of Rho signaling partially rescues the effects of loss of Robo2 function. (**A-B″**) Dorsal views of control GFP+ cells (green) exposed to control pluronic gel (A-A″) or pluronic gel (PL)+ LPA (B-B″). Note the presence of elongating cells and myofibers co-expressing desmin (red; high magnifications in A″ and B″). (**C-C″**) Rb2dN+ cells that received control pluronic gel largely failed to generate fibers (arrowheads in C point to mesenchymal cells and arrow to elongating cell), were randomly distributed both rostral and caudal to the mid-segment (dashed line in C) and lacked desmin (high magnification in C″). (**D-D″**) Rb2dN+ cells exposed to pluronic gel+ LPA were mainly located in the rostral somite half (above the dashed line in D), yet failed to significantly elongate (arrowheads in D point to mesenchymal cells and arrows to elongating cells). Numerous cells co-expressed desmin whereas others remained desmin-negative (D″). Dashed lines subdivide the segment into rostral and caudal halves. (**E**) Quantification of desmin expression and distribution of mesenchymal/elongating pioneers. Error bars represent s.e.m. (**F**) Quantification of the distribution of mesenchymal pioneers to the rostral (R) versus caudal (C) somite halves. Electroporations were at 16-18ss and embryos were fixed 14 hours later. Error bars represent s.e.m. Statistical analysis used the Kruskal-Wallis non-parametric test followed by the Mann-Whitney test for pairwise comparisons.

R lip of each segment towards the opposite pole. Mesenchymal cells that fail to anchor to the R lip might be unfit to differentiate properly. It remains unclear whether, in addition to repellent signals underlying R-C polarity, there exist also chemoattractant cues that direct migration towards the R domain and/or signals that control attachment at the R edges. Surprisingly, no defects were observed when abrogating DM-derived Slit1. Possibly, pioneer cells are particularly sensitive to differences in ligand concentrations present along the R-C extent of the Scl but absent in the DM.

The effects of knocking-down Robo2 or Slit1 were phenocopied by loss of RhoA, but not of RhoB, consistent with only the former being expressed in the early phases of pioneer ontogeny and similar effects were observed when transfecting C3-transferase (O.H.-B., unpublished). Furthermore, RhoA acts downstream of Robo/Slit signaling as activation of endogenous RhoA in Robo2dN-transfected cells significantly rescued cell migration and desmin expression. The observation that RhoA did not rescue fiber formation in the absence of Robo2 activity indicates that additional factors are required downstream of Robo-Slit. In other contexts, Slit-Robo-mediated axonal repulsion was shown to activate RhoA through specific Slit-Robo GTPase activating factors (srGAPs) (Patel and Van Vactor, 2002; Wong et al., 2001). We suggest that in myotomal pioneers, the cytoplasmic domain of Robo2 might similarly interact with srGAPs to recruit RhoA to the membrane and promote its activity. Furthermore, RhoA, through Rho kinase and type 1 phosphatase might be necessary for the assembly and dynamics of desmin filaments (Inada et al., 1999). RhoA, through Rho kinase and type 1 phosphatase was shown to affect the balance between intermediate filament protein phosphorylation and dephosphorylation, thereby affecting the continuous exchange of filament subunits between a soluble and a filamentous state (Inada et al., 1999). Hence, Slit1-Robo2-activated RhoA could be necessary for the assembly and dynamics of desmin filaments in pioneer myoblasts, similar to the effect of RhoA on the polymerization and retrograde flow of actin filaments in other cellular contexts (Edwards et al., 1999; Kardash et al., 2010; Sanders et al., 1999).

Loss of either Robo2, Slit1 or RhoA consistently affected the onset of desmin protein expression in pioneer myoblasts but did not inhibit its transcription, or that of *Myf5* or *MyoD*. In addition, both myogenic genes are also able to upregulate *Robo2* transcription. Taken together, these results suggest that Slit1-Robo2/RhoA act downstream of cell specification to affect the assembly of the desmin cytoskeleton. The precise mechanism by which this is accomplished remains to be investigated. This will be of particular interest as, in contrast to desmin, the onset of myosin expression is not affected by loss of Robo2. Desmin belongs to the family of intermediate filament (IF) proteins (Cooke, 1983; Lazarides and Hubbard, 1976; Small and Sobieszek, 1977). It is the main IF protein of all muscle cells. In avians and mammals, desmin is one of the earliest muscle markers, detected already in epithelial somites and myoblasts (Kaehn et al., 1988; Kahane et al., 1998a; Kaufman and Foster, 1988), where it forms longitudinal filaments associated with the Z-disc (Schroder et al., 2000). Desmin participates in the early establishment of the sarcomere (Furst et al., 1989; Schaart et al., 1989) and its expression precedes that of other proteins of the contractile apparatus, including myosins [this study and Sacks et al. (Sacks et al., 2003)]. Consistent with its roles in connecting the contractile apparatus with mitochondria, nuclei and costamers, knockout embryos exhibit abnormal alignment of myofibrils, disrupted anchorage of myofibrils to the sarcolemma and mitochondria with disturbed function (Bar et al., 2004). We observed that pioneers with either reduced or apparent lack of desmin failed to properly migrate, remained mesenchymal and did not generate fibers. The few cells that partially elongated were abnormally wide and exhibited prominent membrane protrusions, all reflecting abnormal cytoskeletal assembly. Whereas early electroporations abrogated desmin and generated a severe phenotype, late transfections performed after initial desmin expression had no apparent effect on protein immunoreactivity (although it was difficult to assess its relative intensity), and cellular abnormalities were correspondingly less dramatic. It is possible that after initial assembly, desmin filaments are stable and late treatment only impaired polymerization of newly synthesized protein. It is also possible that Robo2-dependent fiber shape and differentiation involves the regulation of additional genes. Along this line, further studies should directly address whether inhibiting desmin recapitulates all or only some of the phenotypes induced by loss of Robo2 function.

Acknowledgements

We thank Yuval Cinnamon for initial expression data of Robo and Slit and for providing Fig. S8 in the supplementary material. We thank S. Guthrie, M. Bronner-Fraser, Z. Yablonka-Reuveni, T. Meyer, G. Prendergast and E. Laufer for reagents. We are indebted to Tallie Bdolach for help with statistics. This study was supported by grants from the Israel Science Foundation (ISF), the EEU 6th Framework program Network of Excellence MYORES, the Association Francaise contre les Myopathies (AFM), and the DFG (SFB 488) to C.K.

Competing interests statement

The authors declare no competing financial interests.

Supplementary material

Supplementary material for this article is available at
http://dev.biologists.org/lookup/suppl/doi:10.1242/dev.065714/-/DC1

References

Adini, I., Rabinovitz, I., Sun, J. F., Prendergast, G. C. and Benjamin, L. E. (2003). RhoB controls Akt trafficking and stage-specific survival of endothelial cells during vascular development. *Genes Dev.* **17**, 2721-2732.

Bar, H., Strelkov, S. V., Sjoberg, G., Aebi, U. and Herrmann, H. (2004). The biology of desmin filaments: how do mutations affect their structure, assembly, and organisation? *J. Struct. Biol.* **148**, 137-152.

Ben-Yair, R. and Kalcheim, C. (2005). Lineage analysis of the avian dermomyotome sheet reveals the existence of single cells with both dermal and muscle progenitor fates. *Development* **132**, 689-701.

Boardman, P. E., Sanz-Ezquerro, J., Overton, I. M., Burt, D. W., Bosch, E., Fong, W. T., Tickle, C., Brown, W. R., Wilson, S. A. and Hubbard, S. J. (2002). A comprehensive collection of chicken cDNAs. *Curr. Biol.* **12**, 1965-1969.

Borman, W. H. and Yorde, D. E. (1994). Barrier inhibition of a temporal neuraxial influence on early chick somitic myogenesis. *Dev. Dyn.* **200**, 68-78.

Bothe, I., Ahmed, M. U., Winterbottom, F. L., von Scheven, G. and Dietrich, S. (2007). Extrinsic versus intrinsic cues in avian paraxial mesoderm patterning and differentiation. *Dev. Dyn.* **236**, 2397-2409.

Brose, K. and Tessier-Lavigne, M. (2000). Slit proteins: key regulators of axon guidance, axonal branching, and cell migration. *Curr. Opin. Neurobiol.* **10**, 95-102.

Buffinger, N. and Stockdale, F. E. (1994). Myogenic specification in somites: induction by axial structures. *Development* **120**, 1443-1452.

Christ, B. and Ordahl, C. P. (1995). Early stages of chick somite development. *Anat. Embryol. (Berl.)* **191**, 381-396.

Christ, B. and Scaal, M. (2008). Formation and differentiation of avian somite derivatives. *Adv. Exp. Med. Biol.* **638**, 1-41.

Christ, B., Jacob, H. J. and Jacob, M. (1978). On the formation of myotomes in embryos. An experimental and scanning electron microscope study. *Experientia (Basel)* **34**, 514-516.

Christ, B., Huang, R. and Scaal, M. (2007). Amniote somite derivatives. *Dev. Dyn.* **236**, 2382-2396.

Cinnamon, Y., Kahane, N. and Kalcheim, C. (1999). Characterization of the early development of specific hypaxial muscles from the ventrolateral myotome. *Development* **126**, 4305-4315.

Cinnamon, Y., Kahane, N., Bachelet, I. and Kalcheim, C. (2001). The sub-lip domain-a distinct pathway for myotome precursors that demonstrate rostral-caudal migration. *Development* **128**, 341-351.

Cinnamon, Y., Ben-Yair, R. and Kalcheim, C. (2006). Differential effects of N-cadherin-mediated adhesion on the development of myotomal waves. *Development* **133**, 1101-1112.

Cooke, P. (1983). Organization of contractile fibers in smooth muscle. *Cell Muscle Motil.* **3**, 57-77.

Denetclaw, W. F., Jr and Ordahl, C. P. (2000). The growth of the dermomyotome and formation of early myotome lineages in thoracolumbar somites of chicken embryos. *Development* **127**, 893-905.

Denetclaw, W. F., Jr, Christ, B. and Ordahl, C. P. (1997). Location and growth of epaxial myotome precursor cells. *Development* **124**, 1601-1610.

Denetclaw, W. F., Jr, Berdougo, E., Venters, S. J. and Ordahl, C. P. (2001). Morphogenetic cell movements in the middle region of the dermomyotome dorsomedial lip associated with patterning and growth of the primary epaxial myotome. *Development* **128**, 1745-1755.

Dickson, B. J. (2001). Rho GTPases in growth cone guidance. *Curr. Opin. Neurobiol.* **11**, 103-110.

Dietrich, S., Schubert, F. R. and Lumsden, A. (1997). Control of dorsoventral pattern in the chick paraxial mesoderm. *Development* **124**, 3895-3908.

Edwards, D. C., Sanders, L. C., Bokoch, G. M. and Gill, G. N. (1999). Activation of LIM-kinase by Pak1 couples Rac/Cdc42 GTPase signalling to actin cytoskeletal dynamics. *Nat. Cell Biol.* **1**, 253-259.

Emerson, M. M. and Van Vactor, D. (2002). Robo is Abl to block N-Cadherin function. *Nat. Cell Biol.* **4**, 227-230.

Furst, D. O., Nave, R., Osborn, M. and Weber, K. (1989). Repetitive titin epitopes with a 42 nm spacing coincide in relative position with known A band striations also identified by major myosin-associated proteins. An immunoelectron-microscopical study on myofibrils. *J. Cell Sci.* **94** 119-125.

Goldstein, R. S. and Kalcheim, C. (1992). Determination of epithelial half-somites in skeletal morphogenesis. *Development* **116**, 441-445.

Gros, J., Scaal, M. and Marcelle, C. (2004). A two-step mechanism for myotome formation in chick. *Dev. Cell* **6**, 875-882.

Gros, J., Manceau, M., Thome, V. and Marcelle, C. (2005). A common somitic origin for embryonic muscle progenitors and satellite cells. *Nature* **435**, 954-958.

Gros, J., Serralbo, O. and Marcelle, C. (2009). WNT11 acts as a directional cue to organize the elongation of early muscle fibres. *Nature* **457**, 589-593.

Groysman, M., Shoval, I. and Kalcheim, C. (2008). A negative modulatory role for Rho and Rho-associated kinase signaling in delamination of neural crest cells. *Neural Dev.* **3**, 27.

Hammond, R., Vivancos, V., Naeem, A., Chilton, J., Mambetisaeva, E., Andrews, W., Sundaresan, V. and Guthrie, S. (2005). Slit-mediated repulsion is a key regulator of motor axon pathfinding in the hindbrain. *Development* **132**, 4483-4495.

Huang, R. and Christ, B. (2000). Origin of the epaxial and hypaxial myotome in avian embryos. *Anat. Embryol. (Berl.)* **202**, 369-374.

Inada, H., Togashi, H., Nakamura, Y., Kaibuchi, K., Nagata, K. and Inagaki, M. (1999). Balance between activities of Rho kinase and type 1 protein phosphatase modulates turnover of phosphorylation and dynamics of desmin/vimentin filaments. *J. Biol. Chem.* **274**, 34932-34939.

Kaehn, K., Jacob, H. J., Christ, B., Hinrichsen, K. and Poelmann, R. E. (1988). The onset of myotome formation in the chick. *Anat. Embryol.* **177**, 191-201.

Kahane, N., Cinnamon, Y. and Kalcheim, C. (1998a). The origin and fate of pioneer myotomal cells in the avian embryo. *Mech. Dev.* **74**, 59-73.
Kahane, N., Cinnamon, Y. and Kalcheim, C. (1998b). The cellular mechanism by which the dermomyotome contributes to the second wave of myotome development. *Development* **125**, 4259-4271.
Kahane, N., Cinnamon, Y., Bachelet, I. and Kalcheim, C. (2001). The third wave of myotome colonization by mitotically competent progenitors: regulating the balance between differentiation and proliferation during muscle development. *Development* **128**, 2187-2198.
Kahane, N., Cinnamon, Y. and Kalcheim, C. (2002). The roles of cell migration and myofiber intercalation in patterning formation of the postmitotic myotome. *Development* **129**, 2675-2687.
Kahane, N., Ben-Yair, R. and Kalcheim, C. (2007). Medial pioneer fibers pattern the morphogenesis of early myoblasts derived from the lateral somite. *Dev. Biol.* **305**, 439-450.
Kalcheim, C. (2000). Mechanisms of early neural crest development: from cell specification to migration. *Int. Rev. Cytol.* **200**, 143-196.
Kalcheim, C., Cinnamon, Y. and Kahane, N. (1999). Myotome formation: a multistage process. *Cell Tissue Res.* **296**, 161-173.
Kardash, E., Reichman-Fried, M., Maitre, J. L., Boldajipour, B., Papusheva, E., Messerschmidt, E. M., Heisenberg, C. P. and Raz, E. (2010). A role for Rho GTPases and cell-cell adhesion in single-cell motility in vivo. *Nat. Cell Biol.* **12**, 47-53.
Kassar-Duchosoy, L., Giacone, E., Gayraud-Morel, B., Jory, A., Gomes, D. and Tajbakhsh, S. (2005). Pax3/Pax7 mark a novel population of primitive myogenic cells during development. *Genes Dev.* **19**, 1426-1431.
Kaufman, S. J. and Foster, R. F. (1988). Replicating myoblasts express a muscle-specific phenotype. *Proc. Natl. Acad. Sci. USA* **85**, 9606-9610.
Kenny Mobbs, T. and Thorogood, P. (1987). Autonomy of differentiation in avian branchial somites and the influence of adjacent tissues. *Development* **100**, 449-462.
Kidd, T., Brose, K., Mitchell, K. J., Fetter, R. D., Tessier-Lavigne, M., Goodman, C. S. and Tear, G. (1998). Roundabout controls axon crossing of the CNS midline and defines a novel subfamily of evolutionarily conserved guidance receptors. *Cell* **92**, 205-215.
Kidd, T., Bland, K. S. and Goodman, C. S. (1999). Slit is the midline repellent for the robo receptor in Drosophila. *Cell* **96**, 785-794.
Kozma, R., Sarner, S., Ahmed, S. and Lim, L. (1997). Rho family GTPases and neuronal growth cone remodelling: relationship between increased complexity induced by Cdc42Hs, Rac1, and acetylcholine and collapse induced by RhoA and lysophosphatidic acid. *Mol. Cell. Biol.* **17**, 1201-1211.
Kramer, S. G., Kidd, T., Simpson, J. H. and Goodman, C. S. (2001). Switching repulsion to attraction: changing responses to slit during transition in mesoderm migration. *Science* **292**, 737-740.
Krull, C. E. (2001). Segmental organization of neural crest migration. *Mech. Dev.* **105**, 37-45.
Kurokawa, K., Nakamura, T., Aoki, K. and Matsuda, M. (2005). Mechanism and role of localized activation of Rho-family GTPases in growth factor-stimulated fibroblasts and neuronal cells. *Biochem. Soc. Trans.* **33**, 631-634.
Lazarides, E. and Hubbard, B. D. (1976). Immunological characterization of the subunit of the 100 A filaments from muscle cells. *Proc. Natl. Acad. Sci. USA* **73**, 4344-4348.
Le Douarin, N. M. and Kalcheim, C. (1999). *The Neural Crest*. New York: Cambridge University Press.
Legg, J. A., Herbert, J. M., Clissold, P. and Bicknell, R. (2008). Slits and Roundabouts in cancer, tumour angiogenesis and endothelial cell migration. *Angiogenesis* **11**, 13-21.
Li, Y., Gonzalez, M. I., Meinkoth, J. L., Field, J., Kazanietz, M. G. and Tennekoon, G. I. (2003). Lysophosphatidic acid promotes survival and differentiation of rat Schwann cells. *J. Biol. Chem.* **278**, 9585-9591.
Morlot, C., Thielens, N. M., Ravelli, R. B., Hemrika, W., Romijn, R. A., Gros, P., Cusack, S. and McCarthy, A. A. (2007). Structural insights into the Slit-Robo complex. *Proc. Natl. Acad. Sci. USA* **104**, 14923-14928.
Münsterberg, A. E. and Lassar, A. B. (1995). Combinatorial signals from the neural tube, floor plate and notochord induce myogenic bHLH gene expression in the somite. *Development* **121**, 651-660.
Münsterberg, A. E., Kitajewski, J., Bumcrot, D. A., McMahon, A. P. and Lassar, A. B. (1995). Combinatorial signaling by Sonic hedgehog and Wnt family members induces myogenic bHLH gene expression in the somite. *Genes Dev.* **9**, 2911-2922.
Ordahl, C. P., Berdougo, E., Venters, S. J. and Denetclaw, W. F., Jr (2001). The dermomyotome dorsomedial lip drives growth and morphogenesis of both the primary myotome and dermomyotome epithelium. *Development* **128**, 1731-1744.
Patel, B. N. and Van Vactor, D. L. (2002). Axon guidance: the cytoplasmic tail. *Curr. Opin. Cell Biol.* **14**, 221-229.
Pertz, O., Hodgson, L., Klemke, R. L. and Hahn, K. M. (2006). Spatiotemporal dynamics of RhoA activity in migrating cells. *Nature* **440**, 1069-1072.
Pownall, M. E., Strunk, K. E. and Emerson, C. P., Jr (1996). Notochord signals control the transcriptional cascade of myogenic bHLH genes in somites of quail embryos. *Development* **122**, 1475-1488.
Relaix, F., Rocancourt, D., Mansouri, A. and Buckingham, M. (2005). A Pax3/Pax7-dependent population of skeletal muscle progenitor cells. *Nature* **435**, 948-953.
Ren, X. D., Kiosses, W. B. and Schwartz, M. A. (1999). Regulation of the small GTP-binding protein Rho by cell adhesion and the cytoskeleton. *EMBO J.* **18**, 578-585.
Rhee, J., Mahfooz, N. S., Arregui, C., Lilien, J., Balsamo, J. and VanBerkum, M. F. (2002). Activation of the repulsive receptor Roundabout inhibits N-cadherin-mediated cell adhesion. *Nat. Cell Biol.* **4**, 798-805.
Ridley, A. J. (2004). Pulling back to move forward. *Cell* **116**, 357-358.
Ridley, A. J. and Hall, A. (1992). Distinct patterns of actin organization regulated by the small GTP-binding proteins Rac and Rho. *Cold Spring Harb. Symp. Quant. Biol.* **57**, 661-671.
Roffers-Agarwal, J. and Gammill, L. S. (2009). Neuropilin receptors guide distinct phases of sensory and motor neuronal segmentation. *Development* **136**, 1879-1888.
Rong, P. M., Teillet, M.-A., Ziller, C. and Le Douarin, N. M. (1992). The neural tube/notochord complex is necessary for vertebral but not limb and body wall striated muscle differentiation. *Development* **115**, 657-672.
Sacks, L. D., Cann, G. M., Nikovits, W., Jr, Conlon, S., Espinoza, N. R. and Stockdale, F. E. (2003). Regulation of myosin expression during myotome formation. *Development* **130**, 3391-3402.
Sanders, L. C., Matsumura, F., Bokoch, G. M. and de Lanerolle, P. (1999). Inhibition of myosin light chain kinase by p21-activated kinase. *Science* **283**, 2083-2085.
Schaart, G., Viebahn, C., Langmann, W. and Ramaekers, F. (1989). Desmin and titin expression in early postimplantation mouse embryos. *Development* **107**, 585-596.
Schroder, R., Furst, D. O., Klasen, C., Reimann, J., Herrmann, H. and van der Ven, P. F. (2000). Association of plectin with Z-discs is a prerequisite for the formation of the intermyofibrillar desmin cytoskeleton. *Lab. Invest.* **80**, 455-464.
Shiau, C. E., Lwigale, P. Y., Das, R. M., Wilson, S. A. and Bronner-Fraser, M. (2008). Robo2-Slit1 dependent cell-cell interactions mediate assembly of the trigeminal ganglion. *Nat. Neurosci.* **11**, 269-276.
Shibata, F., Goto-Koshino, Y., Morikawa, Y., Komori, T., Ito, M., Fukuchi, Y., Houchins, J. P., Tsang, M., Li, D. Y., Kitamura, T. et al. (2008). Robo4 is expressed on hematopoietic stem cells and potentially involved in the niche-mediated regulation of the side population phenotype. *Stem Cells* **27**, 183-190.
Shoval, I., Ludwig, A. and Kalcheim, C. (2007). Antagonistic roles of full-length N-cadherin and its soluble BMP cleavage product in neural crest delamination. *Development* **134**, 491-501.
Small, J. V. and Sobieszek, A. (1977). Studies on the function and composition of the 10-NM(100-A) filaments of vertebrate smooth muscle. *J. Cell Sci.* **23**, 243-268.
Steinbach, O. C., Ulshöfer, A., Authaler, A. and Rupp, R. A. W. (1998). Temporal restriction of MyoD induction and autocatalysis during *Xenopus* mesoderm formation. *Dev. Biol.* **202**, 280-292.
Stern, H. M., Brown, A. M. and Hauschka, S. D. (1995). Myogenesis in paraxial mesoderm: preferential induction by dorsal neural tube and by cells expressing Wnt-1. *Development* **121**, 3675-3686.
Venters, S. J., Thorsteinsdottir, S. and Duxson, M. J. (1999). Early development of the myotome in the mouse. *Dev. Dyn.* **216**, 219-232.
Vermeren, M. M., Cook, G. M. W., Johnson, A. R., Keynes, R. J. and Tannahilll, D. (2000). Spinal nerve segmentation in the chick embryo: analysis of distinct axon-repulsive systems. *Dev. Biol.* **225**, 241-252.
Vivarelli, E. and Cossu, G. (1986). Neural control of early myogenic differentiation in cultures of mouse somites. *Dev. Biol.* **117**, 319-325.
Wang, B., Xiao, Y., Ding, B. B., Zhang, N., Yuan, X., Gui, L., Qian, K. X., Duan, S., Chen, Z., Rao, Y. et al. (2003). Induction of tumor angiogenesis by Slit-Robo signaling and inhibition of cancer growth by blocking Robo activity. *Cancer Cell* **4**, 19-29.
Weiner, J. A., Fukushima, N., Contos, J. J., Scherer, S. S. and Chun, J. (2001). Regulation of Schwann cell morphology and adhesion by receptor-mediated lysophosphatidic acid signaling. *J. Neurosci.* **21**, 7069-7078.
Wong, K., Ren, X. R., Huang, Y. Z., Xie, Y., Liu, G. F., Saito, H., Tang, H., Wen, L., Brady-Kalnay, S. M., Mei, L. et al. (2001). Signal transduction in neuronal migration: Roles of GTPase activating proteins and the small GTPase Cdc42 in the Slit-Robo pathway. *Cell* **107**, 209-221.
Wong, K., Pertz, O., Hahn, K. and Bourne, H. (2006). Neutrophil polarization: spatiotemporal dynamics of RhoA activity support a self-organizing mechanism. *Proc. Natl. Acad. Sci. USA* **103**, 3639-3644.
Yablonka-Reuveni, Z. and Paterson, B. M. (2001). MyoD and myogenin expression patterns in cultures of fetal and adult chicken myoblasts. *J. Histochem. Cytochem.* **49**, 455-462.